Protein Science (1994), *3*:608-619. Cambridge University Press. Printed in the USA.

DNA binding and bending by the transcription factors GAL4(62*) and GAL4(149*)

KARLA K. RODGERS AND JOSEPH E. COLEMAN

Department of Molecular Biophysics and Biochemistry, Yale University, New Haven, Connecticut 06520

(RECEIVED November 19, 1993; ACCEPTED January 25, 1994)

Abstract

The DNA binding domain of the GAL4 transcription factor from yeast is located in the N-terminal 60 residues of the polypeptide of 881 amino acids. This domain binds 2 Zn ions, which form a binuclear cluster, Zn_2C_6, with 6 C residues, two of which bridge the 2 metal ions (Gardner KH et al., 1991, *Biochemistry 30*:11292-11302). Binding of Zn or Cd to GAL4 induces the conformation of the protein necessary to recognize the specific DNA sequence, UAS_G, to which GAL4 binds as a dimer. Gel retardation assays have been utilized to determine the relative affinities of the Zn_2 and Zn_1 forms of the N-terminal 149 residues of GAL4, GAL4(149*), for UAS_G DNA sequences. We show that Cd_2- and Zn_1GAL4(149*) bind to UAS_G DNA with 2-fold and 4-8-fold lower affinities than Zn_2GAL4(149*), respectively. Thus, the metal species and the number of metal ions bound have measurable effects on the specific DNA binding affinity of GAL4, but these differences are small in comparison to the ratio, $>10^3$ under some conditions, that characterizes the specific to nonspecific DNA binding affinities of the N-terminal fragments of GAL4. A shorter N-terminal fragment, GAL4(62*), although it continues to recognize the UAS_G sequence with a high degree of specificity, binds with 1,000-2,000-fold lower affinity than does Zn_2GAL4(149*). Gel retardation titrations of a DNA containing 2 UAS_G sites with increasing concentrations of GAL4(62*) generate a series of 4 retarded bands in contrast to 2 retarded bands formed when the the same DNA is titrated with GAL4(149*). These data suggest that GAL4(62*) binds to the UAS_G sites as individual monomers that dimerize on the DNA, whereas GAL4(149*) binds the UAS_G DNA cooperatively as a dimer. The $\approx 10^3$ lower affinity of GAL4(62*) for the UAS_G DNA can be accounted for by its failure to form dimers in solution. Zn_2-, Zn_1-, or Cd_2GAL4(149*) induces differential rates of gel migration in a series of circularly permutated UAS_G-containing DNA restriction fragments. Analysis of the data suggests that all 3 proteins cause a 26° angle of bend in the DNA when bound to 1 UAS_G site and 45° when bound to 2 tandem UAS_G sites. The same assay shows that GAL4(62*) does not induce significant bending of the UAS_G DNA sequences. Thus, the additional subdomains found in the larger polypeptide fragment, GAL4(149*), must exert an additional force on the DNA either through direct contacts with the DNA or indirectly through altered protein conformation.

Keywords: DNA bending; GAL4; gel shift assay; protein-DNA interactions

GAL4 protein is a transcription factor from *Saccharomyces cerevisiae* required for the transcriptional activation of the genes encoding the galactose-metabolizing enzymes in response to galactose (for review, see Giniger et al., 1985; Johnston, 1987a). The protein of 881 amino acids binds as a dimer to a 17-bp palindromic DNA sequence known as the UAS_G, which is present in 1-4 copies upstream of the inducible genes. In the absence of galactose, GAL4 appears to remain bound to the UAS_G sequence but is inactivated by formation of a complex with another protein, GAL80 (Johnston et al., 1987; Ma & Ptashne, 1987). In the presence of galactose, a metabolite derived from galactose binds to GAL80 altering the interaction between GAL80 and GAL4, thus allowing GAL4 to activate transcription (Leuther & Johnston, 1992). The DNA binding domain of GAL4 is located in the N-terminal 62 residues and includes a sequence, $-C^{11}-X_2-C^{14}-X_6-C^{21}-X_6-C^{28}-X_2-C^{31}-X_6-C^{38}-$, conserved among 21 other fungal transcription factors (see Coleman, 1992, for review). The presence of this Cys-rich sequence initially suggested that GAL4 contained a single "zinc-finger" of the type originally described for TFIIIA (Miller et al., 1985), but with an S_4 rather than an S_2N_2 ligand arrangement (Johnston, 1987b). Analytical data, however, showed that up to 2 metal ions, either Zn(II) or Cd(II), could bind to the 62-residue N-terminal subdomain of GAL4 (Pan & Coleman, 1990a,

Reprint requests to: Joseph E. Coleman, Department of Molecular Biophysics and Biochemistry, Yale University, New Haven, Connecticut 06520; e-mail: coleman@zinc.csb.yale.edu.

1990b). The presence of Zn(II) or Cd(II) was demonstrated to be essential for specific binding of GAL4 to the UAS_G sequence (Pan & Coleman, 1989).

^1H-^{113}Cd coupling patterns observed in 2D ^1H-^1H COSY spectra as well as in ^{113}Cd-filtered ^1H COSY difference spectra of $^{113}Cd_2GAL4(62*)$ have shown that the 6 C residues are the only ligands to the 2 ^{113}Cd ions (Pan & Coleman, 1990a, 1990b; Gadhavi et al., 1991; Gardner et al., 1991). Two of the C residues, C^{11} and C^{28}, were shown to contribute $-S^-$ bridging ligands, confirming the earlier suggestion of a cluster structure based on the chemical shifts of the ^{113}Cd resonances, 707 ppm and 669 ppm, which implied that both $^{113}Cd(II)$ ions were coordinated to 4 sulfur ligands (Pan & Coleman, 1989, 1990a). A crystal structure of the Cd form of the N-terminal 65 residues of GAL4 complexed with a 19-bp UAS_G sequence has confirmed the presence of the binuclear Cd cluster (Kinemage 1; Marmorstein et al., 1992), as has a solution structure of $Cd_2GAL4(65)$ in the absence of DNA at pH 7 done by 2D NMR methods (Baleja et al., 1992). A solution structure of the Zn form of a 43-residue fragment from the DNA binding domain, GAL4(7–49), also shows a conformation compatible with the formation of a Zn binuclear cluster (Kraulis et al., 1992). Although solution data on the Cd forms of the GAL4 N-terminal domain have consistently demonstrated the cooperative binding of 2 Cd ions, the zinc contents of both GAL4(62*) and GAL4(149*) have varied from 1.1 to 2.1 mol zinc/mol protein (Pan, 1990; Pan & Coleman, 1990b). A $Zn_1GAL4(62*)$ gives homogeneous 1D and 2D ^1H NMR spectra, in contrast to the proteins containing an average of 1 ^{113}Cd ion, which show a mixture of the Cd_2 protein and the apoprotein (Pan, 1990).

In order to determine how the specific DNA binding affinity of the DNA binding domain of GAL4 changes as functions of the metal ion content (Zn or Cd), the number of amino acid residues in the N-terminal fragment, the length of the DNA containing the UAS_G palindromic DNA sequence, and the number of tandem UAS_G sequences in the DNA fragment, we have used gel retardation titration methods to determine the binding constants as a function of these variables. Topological changes in the DNA accompanying the binding of the various forms of the GAL4 DNA binding domains have been detected by DNA bending assays.

Results

Binding of Zn_2-, Zn_1-, and $Cd_2GAL4(62*)$ to a consensus UAS_G site

A gel retardation assay of the UAS_G DNA only, a 17-bp fragment, titrated vs. the concentration of $Zn_2GAL4(149*)$ is shown in Figure 1A. From the densitometric analysis of the autoradiogram, the fraction of DNA bound to $Zn_2GAL4(149*)$ was plotted vs. concentration of the protein (Fig. 2A). The plots represent the binding of Zn_2, Zn_1, and Cd_2 forms of GAL4(149*) to the 17-bp isolated UAS_G sequence. All 3 curves are fit well by Equation 1,

$$f_b = DP/D_T = P^n/(K_d{}^n + P^n), \quad (1)$$

where f_b is the fraction of DNA bound, D and P are the DNA and protein concentrations, respectively, and n is the cooperativity parameter. The K_d values calculated according to Equa-

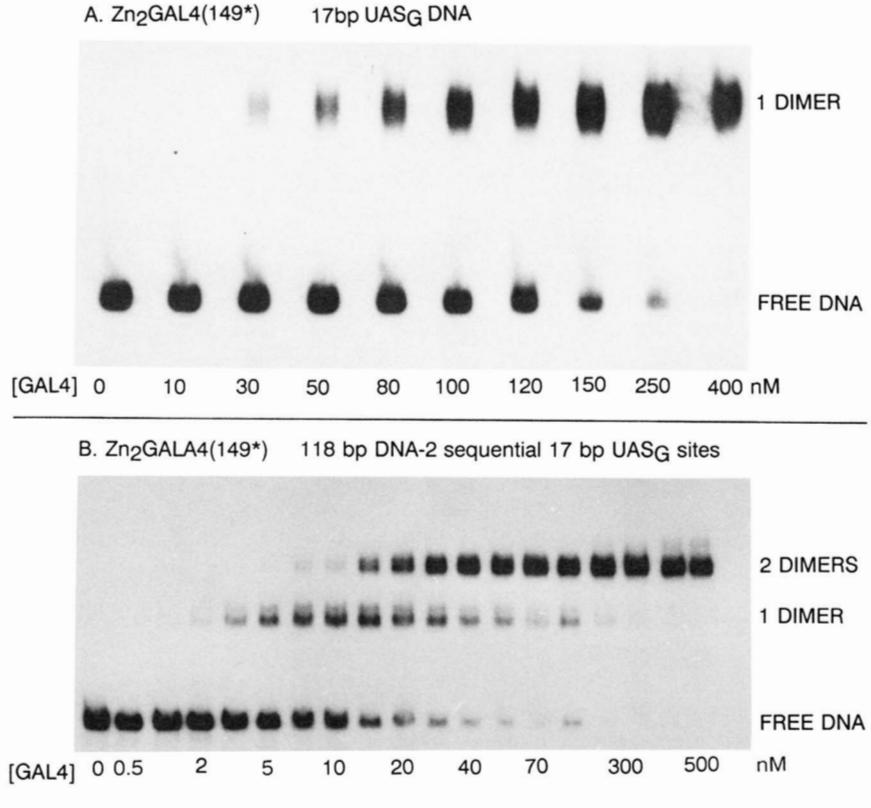

Fig. 1. Gel retardation titration of UAS_G DNA sequences by $Zn_2GAL4(149*)$. **A:** Titration of an isolated 17-bp UAS_G DNA fragment with the indicated concentrations of $Zn_2GAL4(149*)$. The samples were fractionated on a 6% polyacrylamide gel at 25 °C. The concentration of ^{32}P-labeled UAS_G DNA was <10 nm. **B:** Titration of a *Bam* HI-cut 118-bp DNA fragment containing 2 sequential UAS_G sites with $Zn_2GAL4(149*)$. The range of protein concentrations is shown on the bottom of the figure. In addition, the various fractions of DNA are indicated to the right of the figure, including unbound and that complexed with 1 or 2 dimers of $Zn_2GAL4(149*)$. The titration was accomplished using an 8% polyacrylamide gel at 25 °C. The concentration of ^{32}P-labeled 118-bp DNA fragment was <1.0 nM.

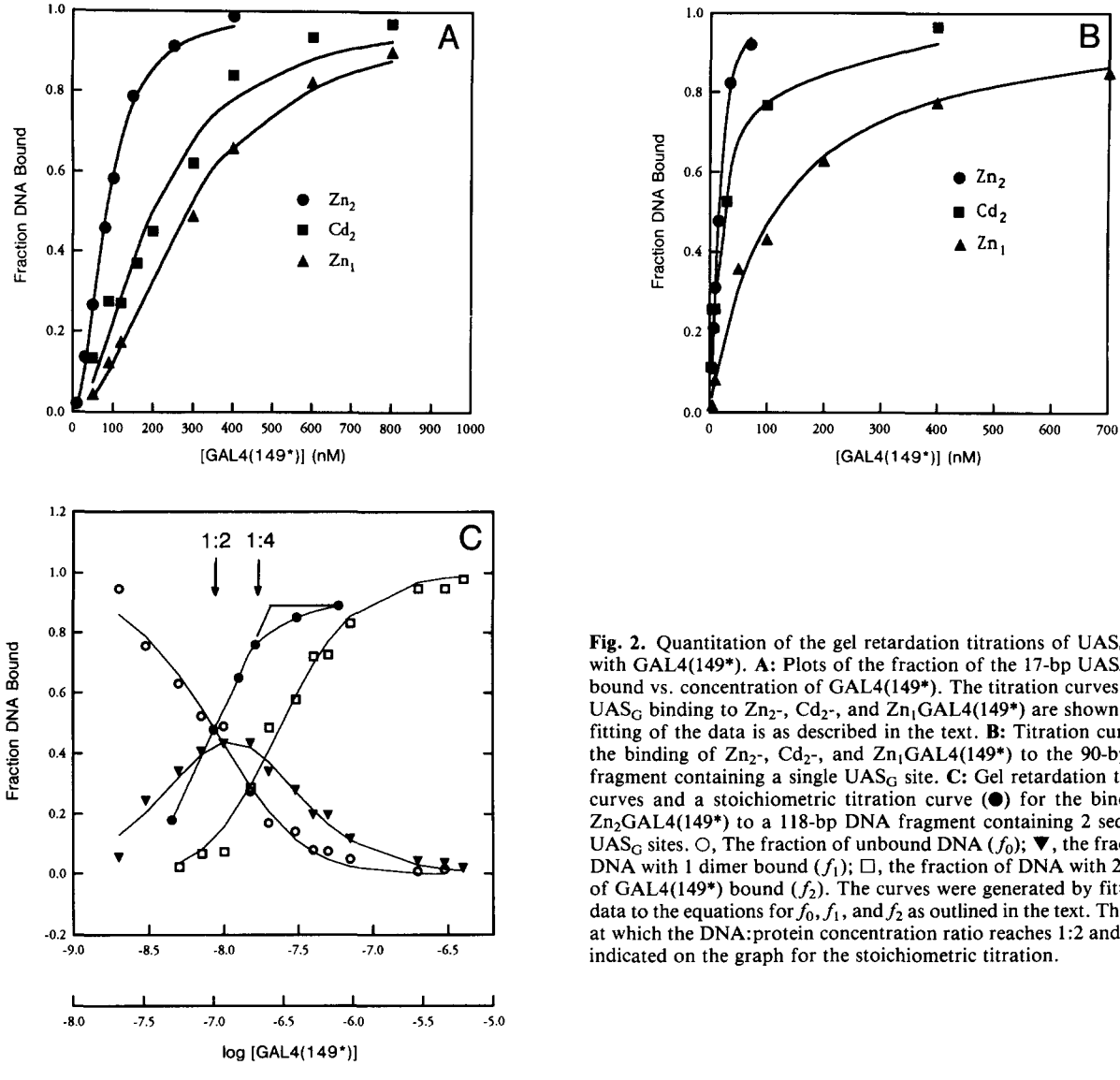

Fig. 2. Quantitation of the gel retardation titrations of UAS_G DNA with GAL4(149*). **A:** Plots of the fraction of the 17-bp UAS_G DNA bound vs. concentration of GAL4(149*). The titration curves for the UAS_G binding to Zn_2-, Cd_2-, and Zn_1GAL4(149*) are shown. Curve fitting of the data is as described in the text. **B:** Titration curves for the binding of Zn_2-, Cd_2-, and Zn_1GAL4(149*) to the 90-bp DNA fragment containing a single UAS_G site. **C:** Gel retardation titration curves and a stoichiometric titration curve (●) for the binding of Zn_2GAL4(149*) to a 118-bp DNA fragment containing 2 sequential UAS_G sites. ○, The fraction of unbound DNA (f_0); ▼, the fraction of DNA with 1 dimer bound (f_1); □, the fraction of DNA with 2 dimers of GAL4(149*) bound (f_2). The curves were generated by fitting the data to the equations for f_0, f_1, and f_2 as outlined in the text. The points at which the DNA:protein concentration ratio reaches 1:2 and 1:4 are indicated on the graph for the stoichiometric titration.

tion 1 are 83 ± 5 nM, 200 ± 10 nM, and 300 ± 12 nM for the complexes of Zn_2-, Cd_2-, and Zn_1GAL4(149*), respectively, with the isolated UAS_G site. For complex formation with all derivatives of GAL4(149*), the best fit of Equation 1 to the data was achieved with $n = 2$.

The K_d for the complex of Zn_2GAL4(149*) formed with a 90-bp fragment containing within it a single UAS_G site is considerably smaller, 13 ± 4 nM. The value of 13 nM is comparable to previous determinations using filter binding assays (Parthun & Jaehning, 1990) and DNase I footprinting analyses (Taylor et al., 1991), all of which employed relatively large DNA fragments. Because the 5′-CCG-3′ triplets of base pairs at each end of the 17-bp UAS_G are the sites of specific interaction with the metal cluster domains, it is possible that end effects reduce the stability of the DNA at the sites most important to the stability of the DNA–protein complex. The binding curves for the Zn_2, Cd_2, and Zn_1 species of GAL4(149*) forming complexes with the 90-bp fragment are compared in Figure 2B. These data are fit with K_d values of 23 ± 4 nM for Cd_2GAL4(149*) and 100 ± 8 nM for Zn_1GAL4(149*), again with $n = 2$. The value of $n = 2$ for a single UAS_G site is reasonable because the dimer of GAL4(149*) is the species expected to bind to a single UAS_G site.

These K_d values describe the specific binding affinity of the GAL4 fragment for the UAS_G DNA sequence in the presence of a large excess of nonspecific DNA. Because this gel system shows no retention of a ^{32}P-labeled nonspecific DNA when added at the same concentration as a UAS_G-containing sequence, Zn_2GAL4(149*) has an apparent affinity for the UAS_G DNA at least 10^3-fold greater than it has for nonspecific DNA. This number is not a direct measure of the difference in affinity constants of GAL4 for specific vs. nonspecific DNA because there is a 10^4 molar excess of unlabeled nonspecific DNA and a relatively low concentration of labeled DNAs to allow the titration to begin in a concentration range where the protein–DNA complex is not fully formed.

Removal of the single zinc ion from the Zn_1GAL4(149*) results in a protein that demonstrates no retardation of a UAS_G-

containing DNA in this gel system (see example in Pan & Coleman, 1989). Readdition of 1 mol Zn/mol protein restores a gel retardation binding isotherm equivalent to that for Zn_1GAL4(149*) produced by dialysis (Fig. 2). Thus the binding of a single zinc ion to the apoGAL4(149*) produces the structural change responsible for restoring at least 3 orders of magnitude in apparent specific DNA binding affinity. In contrast, the binding of the second zinc ion lowers the K_d of the protein-UAS_G complex by only an additional 10-fold.

^{65}Zn and ^{115}Cd binding by GAL4(149) and GAL4(62*)*

At protein concentrations of 1–10 μM for GAL4(62*) and GAL4(149*), it is possible to exchange the intrinsic zinc with the radioactive metal ions ^{65}Zn or ^{115}Cd. These concentrations are within the range used for the gel retardation experiments for GAL4(62*) and at the upper end of the range used for GAL4(149*). Figure 3A illustrates the exchange of ^{65}Zn and ^{115}Cd ions into native GAL4(62*) to produce GAL4(62*) containing 2 ^{65}Zn or 2 ^{115}Cd ions. For both GAL4(62*) and GAL4(149*) a $^{115}Cd_2$ protein is consistently formed reflecting the cooperative binding of 2 Cd ions to the 6 cysteine ligands (Fig. 3A,B). At concentrations of protein and zinc of 100 μM or greater, a Zn_2GAL4(149*) is easily obtained following dialysis against metal-free buffer. However, at concentrations of 10 μM, GAL4(149*) often binds 1 zinc ion (Fig. 3B). On the other hand, Cd readily forms a Cd_2GAL4(149*) at all protein concentrations tested (Fig. 3B). After labeling with 2 metal ions, it is possible to dialyze both proteins at 5–10 μM concentrations with retention of the 2 metal ions. One of the zinc ions, however, can be slowly removed by exhaustive dialysis at these concentrations. The lability of the second zinc is also reflected in the stoichiometry of the Zn forms of both GAL4(149*) and GAL4(62*) if EDTA is used in any of the preparatory buffers (see Pan & Coleman, 1989, 1990b, for zinc analyses of ≈1.5 mol/mol protein).

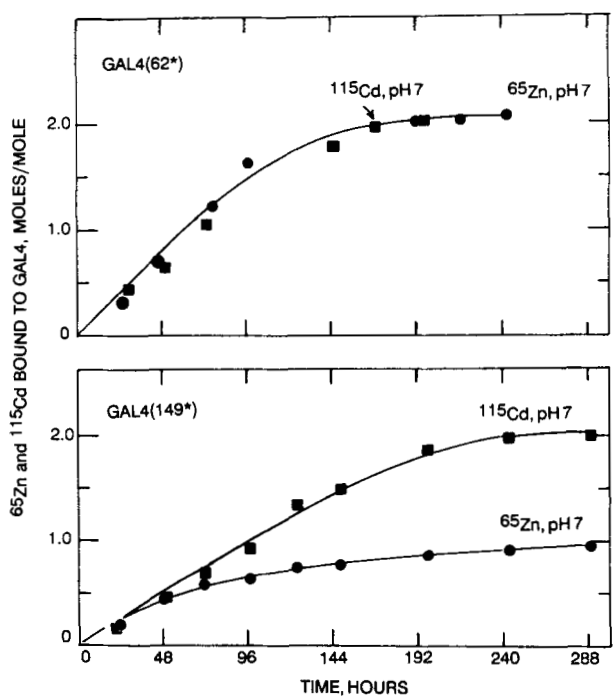

Fig. 3. ^{65}Zn- and ^{115}Cd-labeling of native GAL4(62*) (**A**) and GAL4(149*) (**B**). Conditions were 10 μM proteins contained in 1-mL dialysis bags dialyzed against 50 mL of 10 mM Tris-HCl, 300 mM NaCl, 10 mM β-mercaptoethanol, 10 μM ^{65}Zn (●) or 10 μM ^{115}Cd (■), pH 7.0, 4 °C. The protein-containing bag and a bag containing the buffer alone were counted in a well-type γ-spectrometer (Hewlett-Packard) as a function of time and the difference in cpm between the protein and blank bags converted to mol Zn or Cd bound per mol protein.

Once the $^{65}Zn_2$GAL4(62*) and $^{115}Cd_2$GAL4(62*) species were obtained, it was possible to accurately measure the exchange rates of the central metal ions by dialysis against a 50-fold volume of the corresponding cold metal ion at the same concentration. Exchange experiments for $^{65}Zn_2$GAL4(62*) and $^{115}Cd_2$GAL4(62*) are shown in Figure 4. The most striking observation is that the 2 ^{115}Cd ions of the binuclear cluster exchange with external Cd ions at remarkably different rates, $t_{1/2}$ = 34 h for one and $t_{1/2}$ = 1,350 h for the other. Not unexpectedly for Cd-S coordination, the ^{115}Cd–Cd exchange is much slower than ^{65}Zn–Zn exchange, the latter having a maximum $t_{1/2}$ of ≈96 h. With the observation of the dramatically different exchange rates for the 2 Cd ions, it is probable that the slight break in the Zn exchange curve also indicates 2 exchange rates, one with a $t_{1/2}$ of 24 h and one with a $t_{1/2}$ of 96 h.

Binding of GAL4(149) to multiple UAS_G sites*

Because multiple UAS_G sites exist 5′ to several of the genes activated by GAL4 in *S. cerevisiae*, we investigated the binding of GAL4(149*) to a 118-bp DNA fragment containing 2 sequential UAS_G sites to examine the possibility that GAL4(149*) binds cooperatively to multiple UAS_G sites. Gel retardation titrations of the 118-bp DNA fragment are shown in Figure 1B. This DNA fragment was isolated from a digest of pUASG2 with *Bam* HI, illustrated in Figure 5. The concentration range for the formation of the complex in which a single dimer of GAL4(149*) is bound to one or the other site is overlapping but displaced from that for formation of the complex with dimers of GAL4(149*) bound to each of the 2 sites. Equations 2, 3, and 4 represent the fraction of free DNA, DNA bound to 1 dimer of GAL4(149*), and DNA bound to 2 dimers of GAL4(149*) vs. the concentration of GAL4(149*).

$$f_0 = 1/[1 + (K_1P)^n + (K_2P^2)^n] \quad (2)$$

$$f_1 = (K_1P)^n/[1 + (K_1P)^n + (K_2P^2)^n] \quad (3)$$

$$f_2 = (K_2P^2)^n/[1 + (K_1P)^n + (K_2P^2)^n]. \quad (4)$$

The analyses are as described by Senear and Brenowitz (1991), where P is the protein concentration and n is a cooperativity parameter as in Equation 1, and K_1 and K_2 are association constants.

The fits of the data points for Zn_2GAL4(149*) binding to 2 tandem UAS_G sites (Fig. 1B) to the 3 simultaneous equations are graphed in Figure 2C. The dissociation constant, K_{d1} for binding of a Zn_2GAL4(149*) dimer to 1 UAS_G site is 9.9 ± 4 nM, whereas binding of a second dimer to a UAS_G site adjacent to one already occupied by a GAL4(149*) dimer gives a dissociation constant, K_{d2}, of 20.4 ± 5 nM. If we assume that the

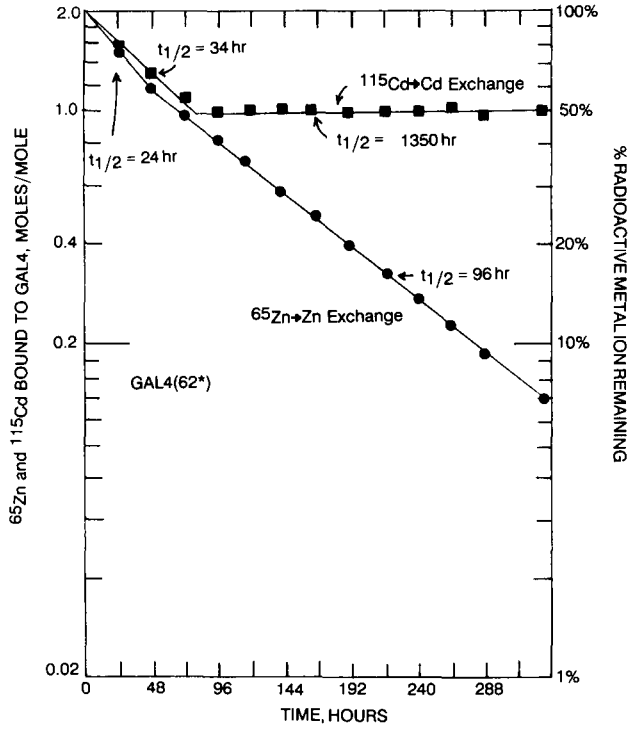

Fig. 4. Exchange of ^{65}Zn (●) and ^{115}Cd (■) in $^{65}Zn_2$GAL4(62*) and ^{115}CdGAL4(62*) for cold Zn or Cd, respectively. Samples of $^{65}Zn_2$GAL4(62*) and $^{115}Cd_2$GAL4(62*) were prepared as described in Figure 3 and then dialyzed against 50 mL of buffer as described in the caption to Figure 3 except it contained 10 μM stable Zn or Cd. The cpm of the protein-containing dialysis bag minus the blank bag were measured as a function of time and converted to mol ^{65}Zn (●) or ^{115}Cd (■) remaining bound to the protein vs. time.

microscopic dissociation constants of GAL4 complexed with either of the 2 UAS_G sites in the 118-bp fragment are identical, then from a statistical analysis the binding of the second dimer should have a dissociation constant (K_{d2}) of 4(K_{d1}) or 39.6 nM if there were no cooperativity of GAL4 binding between the 2 UAS_G sites. However, the second dimer is observed to bind to the remaining UAS_G site with a K_{d2} of 20.4 ± 5 nM (Fig. 1B). Thus there is a small degree of cooperative binding of GAL4(149*) to adjacent UAS_G sites, equating to a free energy of −0.4 kcal/mol. It is of course possible that the free energy of cooperativity may be more substantial with the full-length GAL4 protein as suggested by titrations with full-length GAL4 (Kang et al., 1993). In the case of Cd_2GAL4(149*) binding to the 118-bp DNA fragment, K_{d1} is 26 ± 4 nM and K_{d2} is 85 ± 5 nM. Finally, the

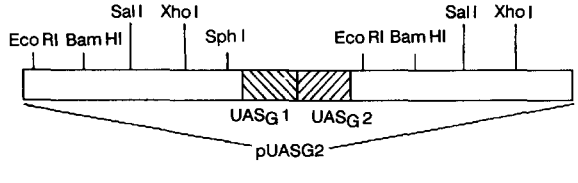

Fig. 5. Schematic illustrating the positions of two UAS_G sequences relative to the restriction endonuclease recognition sites in the plasmid pUASG2.

dissociation constants for the interaction Zn_1GAL4(149*) with the 118-bp fragment are 141 ± 10 nM for K_{d1} and 245 ± 15 nM for K_{d2}. The concentration variation of the free DNA and the 2 GAL4(149*) complexes are accurately fit by the assumption of only 2 binding constants and a cooperativity parameter $n = 2$ (Fig. 2C). This supports the conclusion that 1 preformed GAL4(149*) dimer binds to each UAS_G site (see stoichiometric titration below).

DNA bending assays with GAL4(149)*

In order to examine the possibility that GAL4(149*) induces DNA bending, circularly permutated restriction fragments containing UAS_G sites were used in gel retardation assays as described by Wu and Crothers (1984). Specifically, a vector was designed that contains 2 copies of the UAS_G DNA sequence ligated together without any intervening base pairs. This fragment was then ligated to polylinkers on both ends and inserted into pIBI24. Cutting out this sequence by cleaving the polylinker on both sides with 4 different restriction enzymes, *Eco* RI, *Bam* HI, *Sal* I, and *Xho* I yields four 118-bp DNA fragments in which the tandem UAS_G sites move progressively from the 5′ to the 3′ end of the fragment as shown in Figure 5. Gel retardation assays run simultaneously on all 4 of the restriction fragments at 2 concentrations of Zn_2GAL4(149*), along with a similar gel for Cd_2GAL4(149*), are shown in Figure 6. If GAL4(149*) bends the DNA, the complex with the *Sal* I fragment, containing the 2 UAS_G sites in the center of the 118-bp fragment, should show the greatest retardation as is observed. From the migration of the complex formed with the *Eco* RI-cut fragment (sites at the 3′ end) relative to that of the *Sal* I-cut fragment (sites in the middle) the bending angle can be estimated using Equation 5:

$$\mu m/\mu e = \cos(\alpha/2), \quad (5)$$

where μm is the mobility of the *Sal* I-cut DNA–protein complex, μe is the mobility of the *Eco* RI-cut DNA–protein complex, and α is the angle of DNA bending. This relation was previously determined by comparison with intrinsically bent DNA standards in which bends were induced by the appropriately phased adenine tracts (Thompson & Landy, 1988). For Zn_2GAL4(149*), the calculated bending angles are 26 ± 2° for 1 dimer bound and 45 ± 5° for 2 dimers bound. Model building shows that 2 contiguous 17-bp UAS_G–GAL4 dimer complexes are not completely in phase, thus bends if present should not be strictly additive as observed. These numbers represent a lower limit for the bending angle because the tandem UAS_G sites are not precisely at the end of the *Eco* RI fragment (Fig. 5). Within the error of the measurement, both Cd_2GAL4(149*) and Zn_1GAL4(149*) show the same bending angles as those observed for Zn_2GAL4(149*).

Gel retardation assays of the binding of GAL4(62) to UAS_G sites*

We have found that in order to resolve the bands for GAL4(62*)–UAS_G DNA complexes in a gel retardation assay it is necessary to increase the percentage of polyacrylamide to 20%. Resolution was further improved by reducing the temperature of the running gel to 4 °C in some cases. The gel retardation titrations

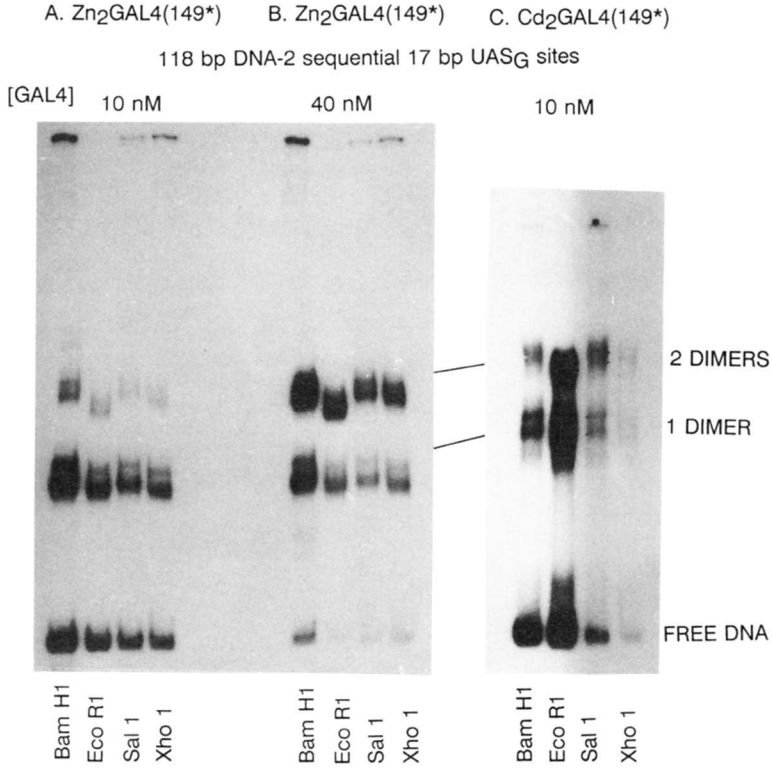

Fig. 6. DNA bending assays with GAL4(149*). **A:** Retention of the four 118-bp DNA fragments (*Bam* HI-, *Eco* RI-, *Sal* I-, and *Xho* I-cut) containing 2 sequential UAS_G sites by 10 nM (**A**) and 40 nM (**B**) $Zn_2GAL4(149*)$. The assay was run on an 8% polyacrylamide gel at 25 °C. **C:** A DNA bending assay analogous to that in part A, with $Cd_2GAL4(149*)$. The fractions of DNA that are unbound and complexed with 1 or 2 dimers of GAL4(149*) are indicated.

of GAL4(62*) with an isolated 17-bp UAS_G fragment illustrate that much larger concentrations of the 62-residue protein are required in order for complex formation to occur as compared with GAL4(149*) (Fig. 7). This gel was run at 25 °C. In contrast to GAL4(149*), there are 2 shifted bands due to protein–DNA complex formation observed on the autoradiogram (Fig. 7).

Four specific protein–DNA bands are formed sequentially upon gel retardation titration with GAL4(62*) using one of the 118-bp DNA fragments containing 2 UAS_G sites and a 20% gel run at 4 °C (Fig. 8A). These same 4 bands are observed in 20% gels run at 25 °C, but the bands are narrower at 4 °C, probably due to a significant decrease in the k_{off}. As further confirmation that the observed retarded bands are due to specific complex formation between GAL4(62*) and the UAS_G sites, we have shown that no detectable protein–DNA bands are observed upon gel retardation titration with GAL4(62*) using a 103-bp DNA fragment containing no UAS_G sites under identical conditions (Fig. 8B).

The precision of data derived from the analyses of the autoradiograms of GAL4(62*) complexes is less than that achieved with GAL4(149*) due to the extremely weak binding of GAL4(62*) and the high percentage acrylamide gels used. Thus the calculated K_d's for the complexes represented by the individual retarded bands have a larger margin of error compared to the analogous results with GAL4(149*). For the binding of GAL4(62*) to the isolated 17-bp UAS_G DNA fragment K_{d1} =

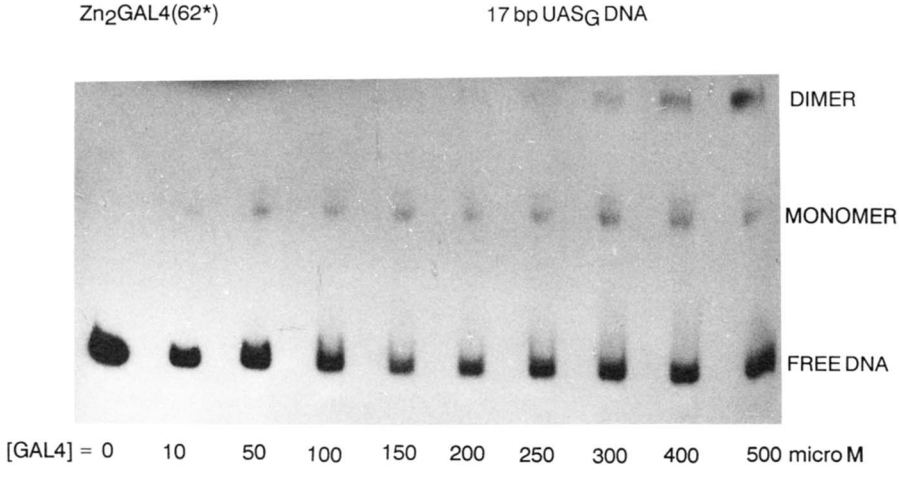

Fig. 7. Gel retardation titration of an isolated 17-bp UAS_G DNA fragment with the indicated concentrations of $Zn_2GAL4(62*)$. The titration was done with a 20% polyacrylamide gel at 25 °C. The concentration of the ^{32}P-labeled 17-bp fragment was <10 nM. The fractions of DNA that are unbound and complexed with a monomer or a dimer of $Zn_2GAL4(62*)$ are indicated in the figure.

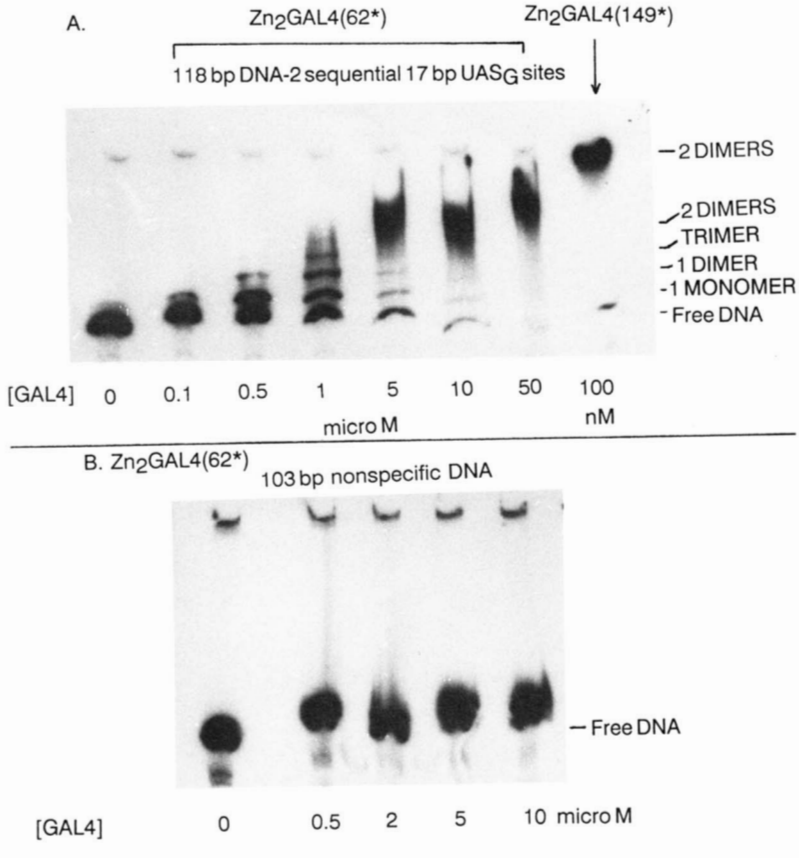

Fig. 8. Gel retardation titrations of specific and nonspecific DNA fragments with $Zn_2GAL4(62*)$. **A:** The titration of a *Bam* HI-cut 118-bp fragment containing 2 sequential UAS_G sites with 0.1–50 μM $Zn_2GAL4(62*)$. The complex of the 118-bp DNA fragment with 2 dimers of $Zn_2GAL4(149*)$ is shown in the far right lane. The fractions of DNA that are free, bound to 1 monomer or 1 dimer, 1 trimer (dimer + monomer) or 2 dimers of $Zn_2GAL4(62*)$ are indicated in the figure. The concentration of the ^{32}P-labeled 118-bp DNA fragment used in the titration is <1 nM. The titration was done using a 20% polyacrylamide gel at 4 °C. **B:** Increasing concentrations of $Zn_2GAL4(62*)$ added to a 103-bp DNA fragment containing no UAS_G sites. The concentration of the ^{32}P-labeled fragment was <1 nM. The titration was done using a 20% polyacrylamide gel at 4 °C. The 103-bp fragment was obtained by digestion of pIBI24 with *Nae* I and *Dra* III. Purification and ^{32}P-labeling of this fragment was done as described in the Materials and methods for the 90-bp and 118-bp DNA fragments.

65 ± 20 μM corresponding to the formation of the most rapidly moving retarded band, and $K_{d2} = 200 \pm 40$ μM corresponding to the formation of the slower moving retarded band (Fig. 7). In the case of GAL4(62*) binding sequentially to 2 UAS_G sites in the 118-bp fragment, the approximate K_d's corresponding to each of the 4 retarded bands in the order of faster to slower migration are $K_{d1} = 4$ μM, $K_{d2} = 8$ μM, $K_{d3} = 10$ μM, and $K_{d4} = 12$ μM. The values given reflect the best fits, but the ranges are relatively large, 1–10 μM for both K_{d1} and K_{d2} and 5–15 μM for both K_{d3} and K_{d4}. Despite much weaker binding to the UAS_G DNA sequence than shown by GAL4(149*), GAL4(62*) still binds the UAS_G sequence with at least 5×10^2-fold higher affinity than nonspecific DNA under the conditions of a large excess of unlabeled DNA based on the range of [GAL4(149*)] used in the experiments of Figure 8.

DNA bending assays with GAL4(62)*

A gel retardation assay (15% acrylamide; 4 °C) of GAL4(62*) at 3 different protein concentrations with the *Eco* RI- and *Sal* I-cut fragments of pUASG2 (Fig. 5) is shown in Figure 9A. If protein-induced DNA bending occurs, the 2 DNA fragments should migrate with the largest differential in the rates of gel migration, because the UAS_G sites are near the end of the *Eco* RI fragment and at the middle of the *Sal* I fragment (Wu & Crothers, 1984). Comparisons of the relative rates of migration of the retarded *Sal* I and *Eco* RI fragments representing all 4 DNA complexes formed with GAL4(62*) show no differences. In contrast, a DNA bending assay of $Zn_2GAL4(149*)$ with the *Eco* RI- and *Sal* I-cut fragments in a 20% acrylamide gel (25 °C) shows a large difference in migration for the *Eco* RI and *Sal* I fragments (Fig. 9B). A comparison of this 20% gel with the 8% gel shown in Figure 6 illustrates the expected increase in the relative difference of migration between the *Eco* RI- and *Sal* I-cut DNA–GAL4(149*) complexes upon the increase in acrylamide concentration.

Protein:DNA stoichiometry within the retarded bands

By increasing the concentration of the UAS_G-containing DNA from 1 nM to 50 nM, we were able to enter a region where a nearly stoichiometric titration of the 2 UAS_G sites in the 118-bp fragments could be carried out with GAL4(149*) in the absence of nonspecific DNA. The 118-bp *Eco* RI fragment (Fig. 5) was additionally cut by *Sph* I to reduce its length to 50-bp (10-bp upstream and 6-bp downstream of the UAS_G sequences) in order to reduce the opportunity for nonspecific binding. As graphed in Figure 2C, a monomer:DNA ratio of 2:1 for $Zn_2GAL4(149*)$ retains 50% of the DNA, whereas 90% of the DNA is retained near a ratio of 4:1. This titration confirms that 2 dimers of $Zn_2GAL4(149*)$ bind to 2 UAS_G sites. Unfortunately it is not practical to increase the DNA concentration sufficiently to carry out a stoichiometric titration with the weakly binding GAL4(62*). Thus we have had to infer the DNA:protein stoichiometry of GAL4(62*) at the UAS_G sites from the structural data which show GAL4(65) to bind to each UAS_G sequence as a dimer (Marmorstein et al., 1992) and the formation of 4 separate complexes on gel retardation (Figs. 8, 9).

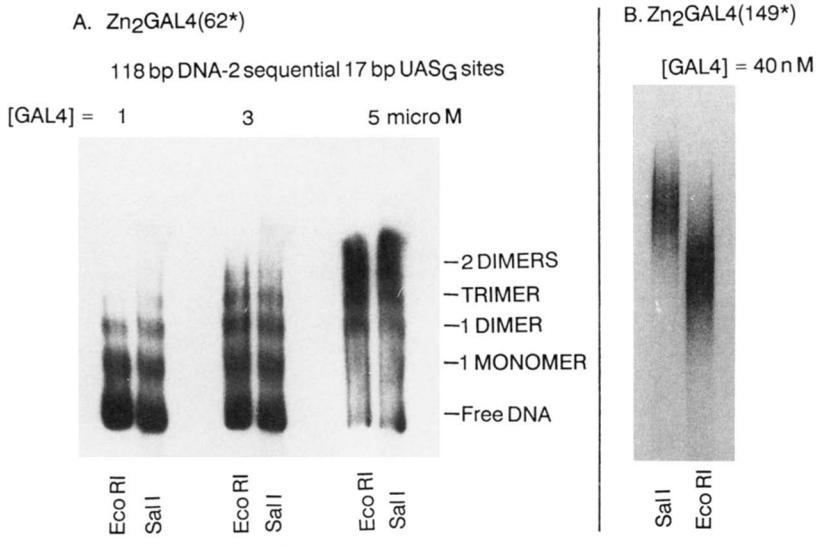

Fig. 9. DNA bending assays with $Zn_2GAL4(62^*)$ and with $Zn_2GAL4(149^*)$ using high percentage polyacrylamide gels. **A:** Retention of ^{32}P-labeled *Eco* RI- and *Sal* I-cut 118-bp DNA fragments containing 2 sequential UAS_G sites with 3 different concentrations of $Zn_2GAL4(62^*)$. The various DNA–protein complexes formed are indicated in the figure. The DNA bending assay was done using a 15% polyacrylamide gel at 4 °C. **B:** Retention of the *Eco* RI- and *Sal* I-cut DNA fragments with $Zn_2GAL4(149^*)$ using a 20% polyacrylamide gel at 25 °C. The band shown represents the 118-bp DNA fragments complexed with 2 dimers of $Zn_2GAL4(149^*)$.

Discussion

The zinc-binding transcription factor, GAL4, has been shown to bind 2 metal ions in a binuclear cluster motif, Zn_2Cys_6. Each metal ion is approximately tetrahedrally coordinated by 4 cysteine ligands, with 2 of the cysteine residues present as bridging ligands between both the metal ions (Pan & Coleman, 1990a, 1990b; Gadhavi et al., 1991; Gardner et al., 1991). Recently, the crystal structure of $Cd_2GAL4(65)$ complexed with a consensus 19-bp UAS_G sequence has been solved to 2.7 Å resolution (Kinemage 1; Marmorstein et al., 1992). Briefly, this structure shows $Cd_2GAL4(65)$ to be bound to the DNA as a symmetrical dimer, with the metal binding subdomain of each monomer making specific contacts with the 3 conserved base pairs (5′-CCG-3′) at either end of the 17-bp UAS_G site. A short helical segment from residue 12 through 17 is positioned such that the C-terminal end points into the major groove of the DNA allowing lysine residues 17 and 18 to make specific contacts with the CCG base pairs. These are the only specific contacts observed between the UAS_G DNA and GAL4(65). A short amphipathic helix (residues 50–64) forms a coiled-coil dimerization subdomain between the 2 monomers. The coiled coil is positioned perpendicular to the axis of the DNA at the center of the UAS_G palindrome (Marmorstein et al., 1992). The metal clusters and dimerization subdomains are linked by residues 41–49, which make minimal nonspecific interactions with the DNA. This results in a fairly exposed region over the middle 11 bp of the UAS_G site.

When we initially examined the spectroscopic properties of the Zn and Cd binuclear clusters formed by GAL4(63) and GAL4(62*) and explored their ability to recognize the GAL4-specific DNA sequence (UAS_G), neither of the shorter fragments formed resolvable bands in standard gel retardation assays (6% acrylamide, 25 °C) (Pan & Coleman, 1990b). The labeled DNA dissociated from the protein during migration in the gel, in marked contrast to the long N-terminal fragment, GAL4(149*), which gave a well-resolved retarded band with UAS_G-containing DNA under the same conditions (Fig. 1A) (Pan & Coleman, 1989). Crosslinking of GAL4(62*) with an avidin–biotin crosslink resulted in the observation of a well-resolved retarded band for the GAL4(62*)–UAS_G complex on a 15% gel, similar to that observed for GAL4(149*) (Pan & Coleman, 1990b). From these observations it was concluded that high specific binding affinity for the palindromic UAS_G DNA sequence by GAL4 or its DNA binding subdomains requires the formation of a dimer in solution. A similar conclusion was reached by Carey et al. (1989), who showed that GAL4(74) has much reduced affinity for the UAS_G sequence compared to GAL4(147), but high affinity could be restored to GAL4(74) if the dimerization domain of the λ repressor was added to the C-terminus (Carey et al., 1989).[1] From the rotationally symmetric contacts made with the UAS_G DNA by GAL4(147) indicated by DNase footprinting and the pattern of binding interference created by ethylation of phosphates, these same investigators concluded that GAL4(147) must bind the UAS_G palindrome as a symmetrical dimer.

The GAL4(147–149) derivatives are widely used as tethers for other protein domains in molecular biological experiments because of their relatively high affinity for a specific DNA sequence. On the other hand, most of the work on structure has been carried out on the GAL4(62–65) derivatives. We therefore sought gel retardation conditions under which complex formation between UAS_G-containing DNA and the unmodified GAL4(62*) could be examined. By employing 15–20% acrylamide gels, it is possible to observe discrete retarded bands formed between UAS_G-containing DNAs and unmodified GAL4(62*) demonstrating that GAL4(62*) specifically recognizes the UAS_G DNA sequence (Figs. 7, 8). The gel retardation titrations provide information about relative affinities and num-

[1] Carey et al. (1989) noted that in vitro cotranslation of 2 GAL4 fragments (1–147 and 1–147 + the C-terminal domain, residues 768–881) yielded an intermediate band upon complex formation with UAS_G DNA from gel retardation analysis, most likely due to the formation of a GAL4 heterodimer. This band was not observed upon simple mixing, prior to gel retardation, of the 2 GAL4 fragments that had been translated separately. It was inferred from these results that the GAL4 fragments form dimers in solution with slow exchange of subunits, such that no appreciable heterodimer is formed unless the 2 fragments are cotranslated.

ber of bound species not readily obtainable by other means, especially for a relatively weakly binding species like GAL4(62*).

Gel retardation assays as a function of protein concentration generate well-behaved binding isotherms for both GAL4(149*) and GAL4(62*), if enough unlabeled nonspecific DNA is added to ensure elimination of all nonspecific binding to the ^{32}P-labeled DNA fragment at the highest protein concentration used (see Materials and methods) (Fig. 2). The gel retardation titrations for GAL4(149*) and GAL4(62*) show the latter to have approximately 10^3 lower affinity than the former for a consensus UAS_G DNA sequence, i.e., K_d's in the μM range for GAL4(62*) vs. the nM range for GAL4(149*) (Figs. 1, 7, 8). When a single UAS_G site is present in the DNA, Zn_2-, Zn_1-, and Cd_2GAL4(149*) all titrate a single retarded band (Figs. 1, 3B). When 2 UAS_G sites are present, 2 major bands are titrated, the first formed migrating faster than the second, and titrating into the second at higher protein concentrations (Figs. 1B, 2C). These gel patterns are compatible with GAL4(149*) binding to 1 isolated UAS_G site as a dimer, whereas 2 adjacent UAS_G sites bind 2 dimers. Only 2 steps are observed in the titration (Fig. 1B), yet the stoichiometric titration shows 4 monomers to be bound to the 2 sites (Fig. 2C).

In contrast, a similar set of gel retardation titrations for GAL4(62*) using the same DNA fragments and 20% gels (at either 25 °C or 4 °C) show the formation of 2 retarded bands for a single 17-bp UAS_G site and 4 retarded bands for the 118-bp fragment containing 2 UAS_G sites (Figs. 7, 8). A model that adequately explains these bands and their titration behavior is one in which the binding process for GAL4(62*) has separated into the sequential binding steps for the individual monomers, each binding to half of the UAS_G palindrome. The faster migration and relative positions of these bands compared to those formed by GAL4(149*) are appropriate for the addition of monomers of the smaller protein to the complex and suggest that the ultimate binding stoichiometry of GAL4(62*) to each UAS_G site is not different from that for GAL4(149*), i.e., 4 monomers to the 2 adjacent UAS_G sites.

The crystal structure of the GAL4(65)-UAS_G complex shows GAL4(65) to bind a single UAS_G sequence as a dimer. However, the multidimensional ^{1}H NMR of GAL4(62*) (Gardner et al., 1991) as well as the solution structure of GAL4(62) determined by 2D and 3D NMR methods (Shirakawa et al., 1993) suggest that GAL4(62-65) derivatives remain monomers in solution up to concentrations >1 mM. Moreover, the dimerization domain from residues 50-60, observed to form a coiled coil in the complex with UAS_G DNA, is unstructured in the free molecule (Shirakawa et al., 1993). Thus, the postulate that GAL4(62*) binds to the UAS_G DNA initially as a monomer followed by dimerization when a second monomer binds to the opposite half of the palindrome is supported by extensive structural data.

Although Cd binds cooperatively to GAL4(149*) and GAL4(62*) to form the Cd_2 species exclusively, ^{115}Cd-Cd exchange shows that one metal site in the binuclear cluster is more stable than the other (Fig. 4). In contrast, an equilibrium exists between the Zn_1 and Zn_2 forms of both GAL4(149*) and GAL4(62*) (Pan, 1990; Gardner et al., 1991). Thus, both Zn_1- and Zn_2GAL4(149*) can be prepared, which allows the demonstration that the GAL4 DNA binding domain specifically recognizes the UAS_G DNA when it contains either 1 or 2 Zn ions; however, formation of the cluster clearly enhances the binding affinity (Fig. 2). NMR spectra of a ^{113}Cd-Zn hybrid of GAL4(149*) and a Zn_2GAL4(149*) partially exchanged with ^{113}Cd suggest that the more weakly bound metal ion in the binuclear cluster is coordinated to cysteines 11, 14, 21, and 28 (Pan, 1990; Pan et al., 1990). Thus, the metal ion in Zn_1GAL4(149*) is probably coordinated to C residues 28, 31, and 38, and a fourth C residue from the N-terminal half of the molecule. If the fourth ligand were C11, the other bridging ligand, induction of similar folding by the binding of 1 Zn could be explained.

Cadmium ions are significantly larger than zinc ions, thus it would seem likely that the protein structure would alter in some manner to accommodate the larger cadmium ions. Indeed, 2D NMR (Gardner et al., 1991) and amide proton exchange results (Mau et al., 1992) are indicative of a more open structure for the Cd_2 form of the protein. Despite these changes, the Cd for Zn substitution results in relatively modest changes in the affinity of the protein for its specific DNA sequence, 2-3-fold, compared to the $\approx 10^3$-fold preference for specific vs. nonspecific DNA under these gel conditions (Fig. 2).

Because GAL4 binds the UAS_G DNA sequence as a dimer, the low concentration of preformed dimers of GAL4(62*) in solution could account for the weak affinity of GAL4(62*) for its specific DNA. If tight dimer formation by GAL4(62*) occurs after binding to the palindromic UAS_G DNA, an unfavorable entropy term will accompany the binding reaction. Assuming that the correct explanation for the 4 retarded bands observed on the gel retardation titration of GAL4(62*) is that the protein binds the DNA as isolated monomers, then the dissociation constant (K_{d1}) for a single GAL4(62*) monomer binding to the 118-bp DNA fragment containing 2UAS_G sites is ≈ 4 μM (−6.8 kcal/mol at 4 °C), whereas K_{d2} for the binding of a second monomer is ≈ 8 μM (−6.4 kcal/mol at 4 °C) (Fig. 8). The binding cycle is modeled in Figure 10. If we assume for the sake of this argument that a dimer of GAL4(62*) in solution would bind to the UAS_G DNA with an affinity similar to that of the dimer of GAL4(149*), then a complex formed with whatever fraction of the GAL4(62*) is a dimer in solution should have a dissociation constant (K_{d3}) of 9.9 nM (−10.9 kcal/mol), the same as measured for GAL4(149*) (Fig. 1B). On the other hand, to complete the thermodynamic cycle of Figure 10, the free energy of

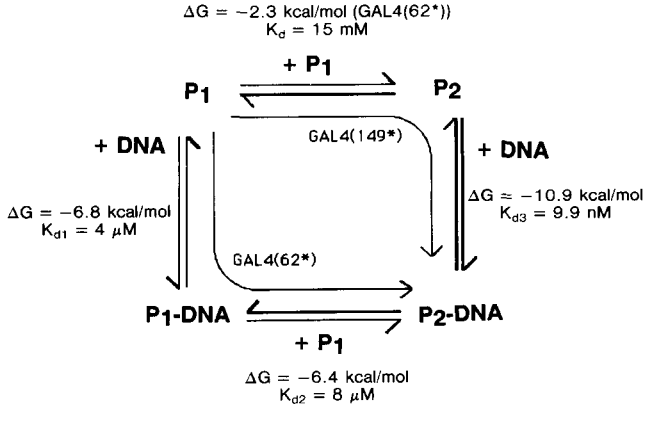

Fig. 10. Thermodynamic cycle of the proposed model for the binding of GAL4(62*) and GAL4(149*) to UAS_G DNA.

dimerization for GAL4(62*) could only be −2.3 kcal/mol based on the measured values of K_{d1}, K_{d2}, and K_{d3} given in Figure 10. This free energy of dimerization has a range of −1.1 to −2.3 kcal/mol if calculated from the analysis of all the data that resolve the binding of GAL4(62*) monomers to the sequential half-sites of the 118-bp fragments as well as the isolated 17-bp UAS_G fragment (Figs. 7, 9). This corresponds to a K_d of 15–155 mM for the dimer of GAL4(62*) in solution, not unreasonable in light of the ^1H NMR data. A calculation of the surface area buried upon formation of the coiled-coil dimerization domain of GAL4(65) bound to the UAS_G in the crystal yields a dimerization energy of −1.8 kcal/mol, assuming −20 cal/mol per Å^2 buried (K. Gardner, unpubl.). Thus, the decrease in binding energy of GAL4(62*) for its specific DNA versus that of GAL4(149*) could be accounted for by the difference in dimerization energies between the 2 species.

The above model does not readily explain why GAL4(149*) induces a conformational change in the UAS_G DNA, which results in changes in the migration of UAS_G-containing circularly permutated DNA fragments usually associated with DNA bending, whereas GAL4(62*) does not (Fig. 9). The differential migration of the *Sal* I and *Eco* RI fragments in the gel bending assay and the large amplification of this difference on a 20% vs. an 8% gel is best explained by a bend in the DNA, ≈26° for 1 dimer of Zn_2GAL4(149*), ≈45° for 2 tandem dimers bound (Figs. 6, 9B). That GAL4(62*) does not induce DNA bending is consistent with conclusions based on the crystal structure of the Cd_2GAL4(65)–UAS_G DNA complex. The latter shows the DNA conformation in the complex to be similar to standard B-DNA structure with only a small degree of bending (≈7°) observed over the 19-bp fragment (Marmorstein et al., 1992). That GAL4(149*) induces a significant topological change in the UAS_G sequence is suggested as well by the observation that if the plasmid pUASG2, containing 2 sequential UAS_G sites, is treated with topoisomerase I, the distribution of topoisomers at equilibrium is substantially altered by the presence of GAL4(149*) compared to the topoisomer distribution observed for the plasmid alone treated with topoisomerase I (unpubl. results). A circular dichroism and ^1H NMR study of a GAL4(1–140)–UAS_G complex by Hansen et al. (1991) was interpreted to show a detectable change in the conformation of the bound nucleic acid. Although the NMR suggested that there was not a major change from a B-type helix, the CD of the bound DNA suggested there was a change in base roll. The latter is expected to be associated with a bend in the DNA (Koo et al., 1986; Crothers et al., 1990). It is possible that a larger dimerization domain of GAL4(149*) could transfer a distorting force to the clusters sufficient to bend the DNA without providing protein–DNA contacts in addition to those present in the GAL4(65)–UAS_G DNA complex. In the crystal structure the dimerization helices are connected to the clusters by 9 residue linkers with relatively large temperature factors. It is therefore difficult to picture a structural basis upon which to support the above hypothesis. The bending could be explained by further contact between distal parts of GAL4(149*) and the exposed 11-bp of DNA in the middle of the UAS_G sequence. Alternatively, more distal parts of the GAL4(149*) may form contacts with the somewhat unstructured 9-residue polypeptide linkers between the dimerization helices and the metal cluster domains, thus making them a more rigid part of the protein molecule. Clearly there must be some caution exercised in extending structural information on small GAL4 subdomains bound to DNA to structure–function relationships assumed for the entire GAL4 protein. DNA bending, as suggested for the larger DNA binding domain of GAL4, could play an important role in the spatial placement, relative to the transcription complex, of the large transactivating domains tethered by relatively small DNA binding domains.

Materials and methods

Purification of GAL4(149) and GAL4(62*)*[2]

Expression of GAL4(149*) was as described previously (Pan & Coleman, 1989, 1990b). Twenty grams of *Escherichia coli* cells containing the plasmid encoding GAL4(149*) were suspended in 40 mL of lysis buffer (50 mM Tris-HCl, pH 8.0, 200 mM KCl, 1 mM EDTA, 1 mM dithiothreitol, 0.2 mM $ZnCl_2$), sonicated twice for 3 min on ice, and centrifuged for 15 min at 5,000 rpm (3,000 × *g*) at 4 °C. Poly(ethylenimine) (Aldrich) was then added over a 10-min period to the lysate on ice to a final concentration of 1%, followed by centrifugation at 15,000 rpm (27,000 × *g*) for 20 min at 4 °C. After dialysis of the supernatant against purification buffer (20 mM Tris-HCl, pH 8.0, 3 mM 2-mercaptoethanol, 10 μM $ZnCl_2$) plus 50 mM NaCl, the dialysate was loaded onto a 12 × 2-cm Trisacryl-SP column (IBF Biotechnics). GAL4(149*) was eluted from the column using a 50–500 mM NaCl gradient in purification buffer. The fractions containing GAL4(149*) were then loaded onto a 10 × 2-cm Bluegel agarose column (Bio-Rad) and eluted with a 200–900 mM NaCl gradient in purification buffer. It is important to add 10–100 μM $ZnCl_2$ to buffers in order to ensure the full zinc content of the final purified protein. Fractions containing GAL4(149*) that were greater than 95% pure, as judged by SDS-PAGE, were pooled.

The purification of GAL4(62*) was identical to that of GAL4(149*) through the Trisacryl-SP column. The fractions containing GAL4(62*) were then dialyzed against purification buffer plus 50 mM NaCl, the dialysate loaded onto a Bluegel agarose column, and eluted with a 50–500 mM NaCl gradient in purification buffer. The fractions containing GAL4(62*) were concentrated to 0.5 mL in an Amicon ultrafiltration apparatus using a YM3 membrane, and loaded onto a 30 × 2-cm P-10 gel filtration column (Bio-Rad) equilibrated with purification buffer plus 100 mM NaCl. The eluted fractions containing GAL4(62*) that were greater than 95% pure were pooled, as judged by SDS-PAGE.

Preparation of Zn_1 and Cd_2 forms of GAL4(149)*

Using the above purification procedure, GAL4(149*) contains 1.6–1.9 Zn(II) per protein molecule. In order to obtain Zn_1GAL4(149*) the protein was dialyzed against 3 L of nitrogen-saturated 20 mM Tris-HCl (pH 7.5), 3 mM 2-mercaptoethanol, 100 mM NaCl, 3 mM EDTA solution at 4 °C for 17 h. The same species can be obtained by preparing the apoGAL4(149*)

[2] GAL4(62*) refers to a cloned protein fragment of GAL4 containing the N-terminal 60 residues of the protein plus 2 C-terminal residues (L-D) from the cloning vector vs. L-E in the native protein. GAL4(149*) is a cloned protein fragment containing the N-terminal 147 residues of the protein plus 2 C-terminal residues (L-D) from the cloning vector vs. I-D in the native protein (Pan, 1990).

or apoGAL4(62*) as previously described (Pan & Coleman, 1989; Pan, 1990) and adding back 1 mol Zn/mol protein. Cd_2GAL4(149*) was produced by dialysis of native protein against 3 L of nitrogen-saturated 0.1 mM $CdCl_2$, 20 mM Tris-HCl (pH 7.5), 3 mM 2-mercaptoethanol, 100 mM NaCl solution at 4 °C for 17 h, followed by dialysis against metal-free buffer.

Protein concentrations and metal analyses

As described previously (Gardner et al., 1991), it is necessary to use amino acid analyses to determine accurate protein concentrations of GAL4. These analyses were used to determine the ϵ_{280nm} for the various species of GAL4(149*) and GAL4(62*). They are as follows: Zn_2GAL4(62*) = 7.8×10^3 M^{-1} cm^{-1}, Zn_2GAL4(149*) and Zn_1GAL4(149*) = 7.3×10^3 M^{-1} cm^{-1}, and Cd_2GAL4(149*) = 11×10^3 M^{-1} cm^{-1}. Zn and Cd concentrations were obtained by atomic absorption spectroscopy using an Instrumentation Laboratory (Lexington, Massachusetts) IL157 spectrometer. The metal contents of the Zn_2, Zn_1, and Cd_2 forms of the N-terminal domains of GAL4 were measured on solutions of 1–10 μM corresponding to the calibration curve for the atomic absorption spectrometer. Measurements of stock solutions of protein varying from 100 μM to 1 mM were performed by making the required dilution immediately before measurement. Metal contents were confirmed by equilibrium dialysis using radioactive ^{65}Zn and ^{115}Cd for protein concentrations from 5–30 μM.

Construction of plasmids

The plasmid pUASG1 contains a single consensus UAS_G site. This was prepared by ligating the annealed oligonucleotides

```
5'-GATCC CGGAAGACTCTCCTCCG G
         G GCCTTCTGAGAGGAGGC CCTAG-5'
```

into pIBI24, which had been previously digested with *Bam* HI. The plasmid pUASG2 contains 2 sequential UAS_G sites flanked on either side by identical polylinker regions. This was obtained by ligating a DNA sequence containing 2 tandem UAS_G consensus sites to polylinkers on both ends and inserting the resulting fragment into pIBI24. A diagram of this region of pUASG2 is shown in Figure 5.

Preparation and radiolabeling of DNA fragments

Gel retardation assays were done with 3 different DNA fragments; an isolated 17-bp UAS_G consensus site, a 90-bp DNA fragment containing a single UAS_G site, and 4 118-bp DNA fragments each containing 2 sequential UAS_G sites. The isolated UAS_G site was prepared by annealing the 2 synthetic oligonucleotides shown below.

```
CGGAAGACTCTCCTCCG
GCCTTCTGAGAGGAGGC
```

This DNA fragment was ^{32}P-labeled with [γ-^{32}P]ATP using T4 polynucleotide kinase (New England Biolabs). The 90-bp DNA fragment was obtained by digesting pUASG1 with *Eco* RI and *Hind* III. The DNA fragment was purified by standard techniques and ^{32}P-labeled with [α-^{32}P]dATP using the large (Klenow) fragment of *E. coli* DNA polymerase I (New England Biolabs). The 118-bp fragments containing 2 sequential UAS_G sites were obtained by digesting pUASG2 with either *Bam* HI, *Eco* RI, *Sal* I, or *Xho* I (Fig. 5). After purification these DNA fragments were labeled as described for the 90-bp fragment.

Gel retardation assays

Gel retardation assays of GAL4(149*) with the UAS_G DNA sequences were performed on 6–20% polyacrylamide gels at 25 °C by standard techniques (Fried & Crothers, 1981). The acrylamide to bisacrylamide ratio in the stock solution was 37.5:1. The assays with GAL4(62*) were done on 15 or 20% polyacrylamide gels and in some cases were run at 4 °C. In all cases the sample buffer contained 10 mM Tris-HCl (pH 7.5), 50 mM KCl, 5 mM $MgCl_2$, 1 mM dithiothreitol, 1–3 μg calf thymus DNA (Sigma), and 6% glycerol. The nonspecific calf thymus DNA was titrated into the samples to assure that no retention of a ^{32}P-labeled, non-UAS_G-containing DNA was observed on the gel using the highest concentration of the GAL4 protein fragments. We determined that a 10^4 molar excess of unlabeled calf thymus DNA was required to suppress "ladder-like" bands appearing at the high protein concentration ends of these titrations on the longer UAS_G-containing DNAs due to nonspecific binding of the GAL4 derivatives outside the UAS_G sequence. In addition, the binding isotherms can be subtly distorted by nonspecific complexes that overlie the specific complexes at concentrations of protein where the nonspecific "ladders" are not yet apparent.

The assays were done using an SE600 series Hoeffer gel apparatus with 45 mM Tris-borate as the electrophoresis buffer. After electrophoresis the gels were dried and exposed to Kodak XAR-5 film. A series of exposures were run for each gel to select the range of exposure over which the densitometry generated the same binding curves. The resulting autoradiograms were analyzed using a Hoeffer GS300 scanning densitometer.

A "dilution assay" as described in Liu-Johnson et al. (1986) was performed to determine the fraction of the GAL4 molecules participating in binding and to assure that large variations did not occur between preparations. This assay plots gel retardation data obtained at several total DNA and protein concentrations, but the same DNA:protein ratios, according to the following equation: $(1 - r)(\alpha - r)/r = 1/K(1/DNA_{tot})$ where r is the fraction of ^{32}P-DNA bound and α is the ratio of active protein to DNA. Alpha is determined by adjusting the line so that the y ordinate is zero. This analysis for GAL4(149*) and GAL4(62*) show the fraction of active GAL4 to be $\approx$0.9.

^{65}Zn and ^{113}Cd exchanges

^{65}Zn and ^{113}Cd exchanges into GAL4(62*) and GAL4(149*) were carried out in 1-mL dialysis bags suspended in 50 mL of exchange buffer as described previously (Coleman & Vallee, 1960). Concentrations of GAL4(149*) and GAL4(62*) used in the equilibrium dialysis studies varied from 5 to 30 μM.

Acknowledgments

This study was supported by NIH grants GM21919 and DK09070.

References

Baleja JD, Marmorstein R, Harrison SC, Wagner G. 1992. Solution structure of the DNA binding domain of Cd_2-GAL4 from *S. cerevisiae*. *Nature (Lond) 356*:450–453.

Carey M, Kakidani H, Leatherwood J, Mostashari F, Ptashne M. 1989. An amino terminal fragment of GAL4 binds DNA as a dimer. *J Mol Biol 209*:423–432.

Coleman JE. 1992. Zinc proteins: Enzymes, storage proteins, transcription factors, and replication proteins. *Annu Rev Biochem 61*:897–946.

Coleman JE, Vallee BL. 1960. Metallocarboxypeptidases. *J Biol Chem 235*:390–395.

Crothers DM, Haran TE, Nadeau JG. 1990. Intrinsically bent DNA. *J Biol Chem 265*:7093–7096.

Fried M, Crothers DM. 1981. Equilibria and kinetics of lac repressor-operator interactions by polyacrylamide gel electrophoresis. *Nucleic Acids Res 9*:6505–6525.

Gadhavi PL, Davis AL, Povey JF, Keeler J, Laue ED. 1991. Polypeptide-metal cluster connectivities in Cd(II)GAL4. *FEBS Lett 281*:223–226.

Gardner KH, Pan T, Narula S, Rivera E, Coleman JE. 1991. Structure of the binuclear metal-binding site in the GAL4 transcription factor. *Biochemistry 30*:11292–11302.

Giniger E, Varnum SM, Ptashne M. 1985. Specific DNA binding of GAL4, a positive regulatory protein of yeast. *Cell 40*:767–774.

Hansen A, Van Hoy M, Kodadek T. 1991. Spectroscopic studies of the DNA binding site of the GAL4 "zinc finger" protein. *Biochem Biophys Res Commun 175*:492–499.

Johnston M. 1987a. A model fungal gene regulatory mechanism: The GAL genes of *Saccharomyces cerevisiae*. *Microbiol Rev 51*:458–476.

Johnston M. 1987b. Genetic evidence that zinc is an essential co-factor in the DNA binding domain of GAL4 protein. *Nature (Lond) 328*:353–355.

Johnston SA, Salmeron JM, Dincher SS. 1987. Interaction of positive and negative regulatory proteins in the galactose regulon of yeast. *Cell 50*:143–146.

Kang T, Martins T, Sadowski I. 1993. Wild type GAL4 binds cooperatively to GAL1-10 UAS_G in vitro. *J Biol Chem 268*:9629–9635.

Koo HS, Wu HM, Crothers DM. 1986. DNA bending at adenine–thymine tracts. *Nature (Lond) 320*:501–506.

Kraulis PJ, Raine ARC, Gadhavi PL, Laue ED. 1992. Structure of the DNA-binding domain of zinc GAL4. *Nature (Lond) 356*:448–450.

Leuther KK, Johnston SA. 1992. Nondissociation of GAL4 and GAL80 in vivo after galactose induction. *Science 256*:1333–1335.

Liu-Johnson HN, Gartenberg MR, Crothers DM. 1986. The DNA binding domain and bending angle of *E. coli* CAP protein. *Cell 47*:995–1005.

Ma J, Ptashne M. 1987. Deletion analysis of GAL4 defines two transcriptional activating segments. *Cell 48*:847–853.

Marmorstein R, Carey M, Ptashne M, Harrison SC. 1992. DNA recognition by GAL4: Structure of a protein-DNA complex. *Nature (Lond) 356*:408–414.

Mau T, Baleja JD, Wagner G. 1992. Effects of DNA binding and metal substitution on the dynamics of the GAL4 DNA-binding domain as studied by amide proton exchange. *Protein Sci 1*:1403–1412.

Miller J, MacLachlan AD, Klug A. 1985. Repetitive zinc-binding domains in the protein transcription factor IIIA from *Xenopus* oocytes. *EMBO J 4*:1609–1614.

Pan T. 1990. Structure and function of the Zn(II) binding sites within the DNA binding domains of the GAL4 and the mammalian glucocorticoid receptor proteins [thesis]. New Haven, Connecticut: Yale University.

Pan T, Coleman JE. 1989. Structure and function of the Zn(II) binding site within the DNA binding domain of the GAL4 transcription factor. *Proc Natl Acad Sci USA 86*:3145–3149.

Pan T, Coleman JE. 1990a. GAL4 transcription factor is not a "zinc finger" but forms a $Zn(II)_2Cys_6$ binuclear cluster. *Proc Natl Acad Sci USA 87*:2077–2081.

Pan T, Coleman JE. 1990b. The DNA binding domain of GAL4 forms a binuclear metal ion complex. *Biochemistry 29*:3023–3029.

Pan T, Halvorsen YD, Dickson RC, Coleman JE. 1990. The transcription factor LAC9 from *Kluyveromyces lactis* like GAL4 from *Saccharomyces cerevisiae* forms a $Zn(II)_2Cys_6$ binuclear cluster. *J Biol Chem 265*:21427–21429.

Parthun MR, Jaehning JA. 1990. Purification and characterization of the yeast transcriptional activator GAL4. *J Biol Chem 265*:209–213.

Senear DF, Brenowitz M. 1991. Determination of binding constants for cooperative site-specific protein-DNA interactions using the gel mobility-shift assay. *J Biol Chem 266*:13661–13671.

Shirakawa M, Fairbrother WJ, Serikawa Y, Ohkubo T, Kyogoku Y, Wright PE. 1993. Assignment of ^1H, ^{15}N and ^{13}C resonances, identification of elements of secondary structure and determination of the global fold of the DNA-binding domain of GAL4. *Biochemistry 32*:2144–2153.

Taylor ICA, Workman JL, Schuetz TJ, Kingston RE. 1991. Facilitated binding of GAL4 and heat shock factor to nucleosomal templates: Differential function of DNA binding domains. *Genes & Dev 5*:1285–1298.

Thompson JF, Landy A. 1988. Empirical estimation of protein-induced DNA bending angles: Applications to λ site-specific recombination complexes. *Nucleic Acids Res 5*:9687–9705.

Wu HM, Crothers DM. 1984. The locus of sequence-directed and protein-induced DNA bending. *Nature (Lond) 308*:509–513.